Full and Partial Crosswalls Between Unit Cells of Endfire Slotline Arrays

Gregory J. Wunsch, *Member, IEEE* and Daniel H. Schaubert, *Fellow, IEEE*

***Abstract*—Endfire slotline antenna arrays, also known as Vivaldi notch arrays, may be used to build broad-band phased arrays with wide scanning capabilities. However, scan blindnesses may render the phased array unusable over portions of its intended operating frequency range and scan volume. One such scan blindness occurs in the E-plane of single polarized arrays and can be predicted by a simple formula. By inserting full and partial crosswalls between unit cells of the array, this blindness can be moved to higher frequencies, moved toward endfire, or totally eliminated. Arrays with upper crosswalls exhibit another type of scan blindness. This scan blindness can be utilized to reduce far-out sidelobes of a limited-scan array.**

***Index Terms*—Electromagnetic surface waves, phased arrays, scan blindness, sidelobe suppression, Vivaldi notch arrays.**

I. Introduction

BROAD-BAND phased-array antennas with wide scanning capabilities may be built by using endfire slotline antennas as array elements. This type of array was proposed by Lewis *et al.* [1] in 1974. Small endfire slotline antenna arrays are depicted in Fig. 1. A stripline feed embedded in the dielectric couples energy to the slotlines printed on each side of the dielectric (Fig. 2). This is known as the bilateral configuration. The width of the slotlines increases near the edge of the dielectric. The transmitted wave travels down the slotline toward the edge, where it launches into free-space. The widened portion of the slotline can take a number of different shapes [2]–[5]. Microstrip feeds coupling to slotlines in the unilateral configuration (slotlines printed on only one side of the dielectric substrate) are also possible, [6] for instance.

It is clear that the authors of [1] introduced this antenna primarily as an array element, although the single element is useful by itself. The arrays analyzed in this paper are single-polarized infinite planar arrays backed by a ground plane. The ground plane is needed to prevent radiation in the backward direction, which will occur if the H-plane spacing exceeds one-half wavelength. The elements are located in a rectangular grid. Fig. 1(a) shows a small ordinary array (without crosswalls) above a ground plane. Fig. 1(b) shows the small array with full crosswalls inserted between unit cells.

When the notch antenna is used in the array environment, scan blindnesses and resonances can occur, rendering the phased array unusable over portions of the intended frequency range and scan volume. These catastrophic effects are not easily predicted. They usually become apparent only during prototyping or computer simulation of the proposed array. An E-plane scan blindness can occur when the H-plane spacing exceeds one half of a free-space wavelength [7]. Equations that predict the blind angle, given the frequency and array geometry, are provided in [8]. A surface wave traveling down the trough formed by the metallization on the dielectric and the ground plane (Fig. 3) provides the physical mechanism on which these equations are based. The criterion requiring H-plane spacing greater than one-half wavelength is not usually met for arrays that scan in that plane, but arrays that scan in the E-plane only often have H-plane spacings of approximately 0.75 wavelengths.

This paper investigates the effects of inserting full and partial metallic crosswalls between unit cells. These crosswalls are in-

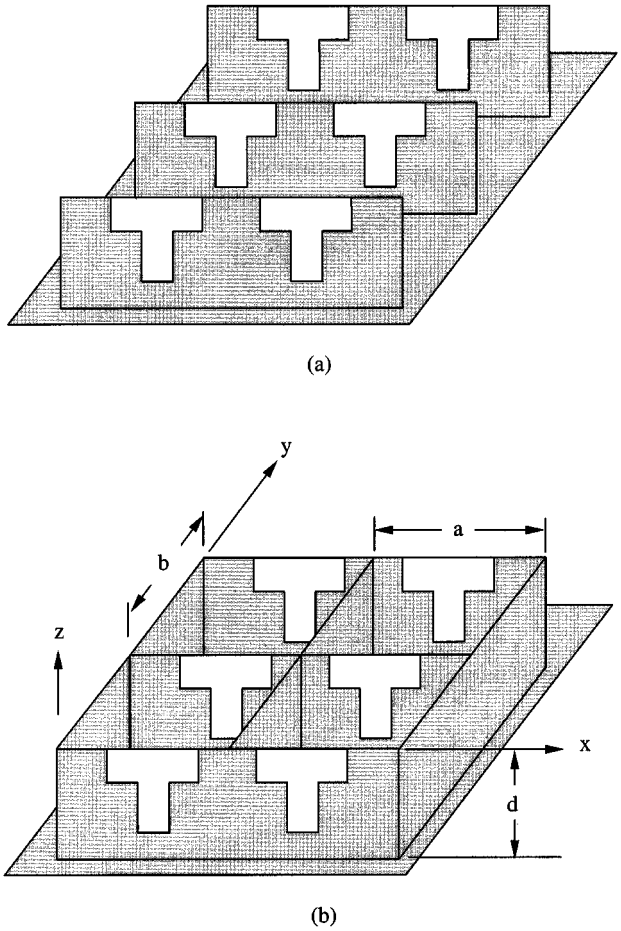

Fig. 1. Small arrays (a) without crosswalls and (b) with full crosswalls.

Manuscript received August 5, 1998; revised February 18, 2000. This work was supported in part by the U.S. Army Research Office under Grant DAAH-94-G-0138.

The authors are with the Electrical and Computer Engineering Department, University of Massachusetts, Amherst, MA 01003 USA.

Publisher Item Identifier S 0018-926X(00)05787-2.

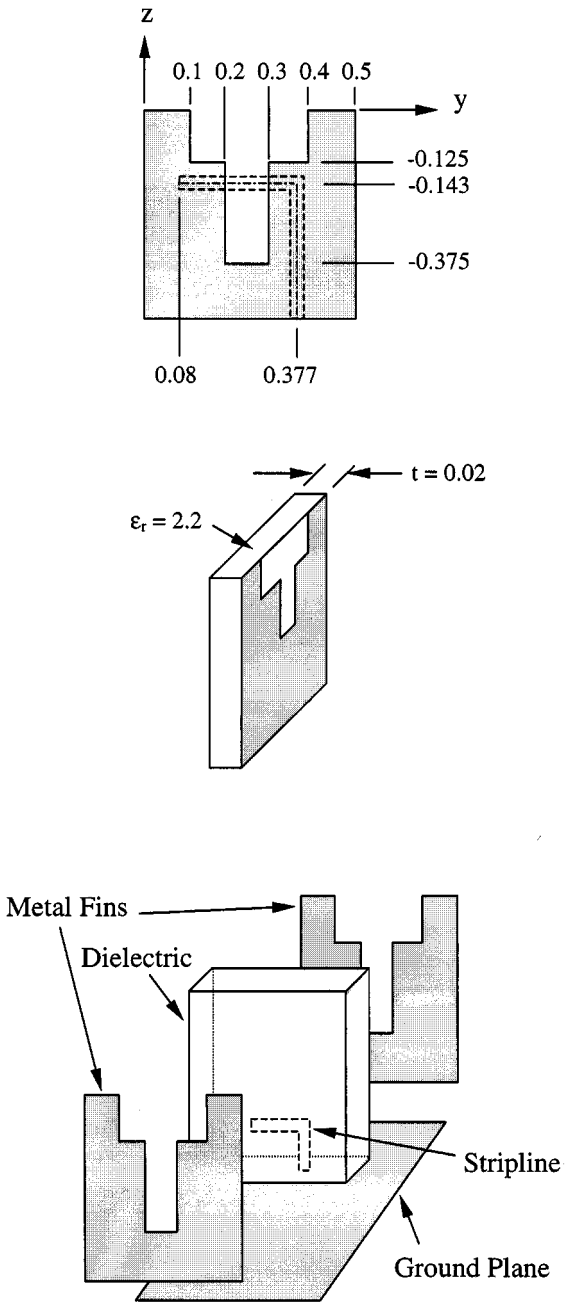

Fig. 2. Slotline antenna used in these simulations. E-plane element spacing in array $= 0.5$ cm. H-plane spacing $= 0.62$ cm. All dimensions in centimeters.

tended to obstruct the path of the surface wave. A full-wave moment method computer code capable of modeling these arrays with crosswalls was used to obtain the active element patterns. This paper contains broad-band (10 to 45 GHz) E-plane scan patterns, which are computed for the array with no crosswalls, full walls, lower walls, and upper walls. Single-frequency patterns for these arrays were presented in [9].

II. Method of Simulation

A full-wave moment-method computer program was developed that is capable of simulating full and partial crosswalls between unit cells of these arrays. A complete description of the simulation method can be found in [10]. It is similar to those described in [11] and [12], but has metallic crosswalls included as part of the unit cell structure, as in [13]. Additionally, this program allows sheets of magnetic current to be placed upon the metallic crosswall, simulating openings in this wall by the equivalence principle. If these current sheets cover the entire crosswall, the structure reverts to the structures described in [11] and [12]. As in [11]–[13], the analysis utilizes the equivalence principle, resulting in unknown equivalent currents at the array aperture ($\mathbf{J}^{\rm ap}$), in the slotline and on the crosswalls (M^s), and on the stripline feed (J^s). In this implementation, the basis functions representing $\mathbf{J}^{\rm ap}$ are Floquet modes, described below. The code solves the infinite array problem for currents on the stripline feed, slotline, crosswall, and aperture. Excitation of the system is provided by a delta gap generator at the ground plane end of the stripline feed. Using the values of the currents, the active element impedance at the stripline feed point can be determined. The active element pattern is computed as

$$P_a(\theta,\phi) = (1 - |\Gamma(\theta,\phi)|^2)\cos\theta$$

where $\Gamma(\theta,\phi)$ is the reflection coefficient looking into the stripline feed.

This computer program evaluates moment method matrix elements using Green's functions. The Green's functions that relate to fields in the region $z < 0$ are represented by double infinite summations, so the matrix elements also require double infinite summations [10]. To calculate numerical values, both summations were truncated at the same value N_a.

The aperture current sheets that relate to radiation in the region $z > 0$ are expanded as

$$\mathbf{J}^{\rm ap} = \hat{\mathbf{x}} \sum_{m=-N_f}^{N_f} \sum_{n=-N_f}^{N_f} I_x^{\rm ap}(m,n) B_x^{\rm ap}(m,n) + \hat{\mathbf{y}} \sum_{m=-N_f}^{N_f} \sum_{n=-N_f}^{N_f} I_y^{\rm ap}(m,n) B_y^{\rm ap}(m,n)$$

where

$$B_x^{\rm ap}(m,n) = e^{-j(U_m x + V_n y)}/b$$
$$B_y^{\rm ap}(m,n) = e^{-j(U_m x + V_n y)}/a,$$
$$U_m = k_0 \sin\theta_0 \cos\phi_0 + \frac{2\pi m}{a}$$
$$V_n = k_0 \sin\theta_0 \sin\phi_0 + \frac{2\pi n}{b}$$

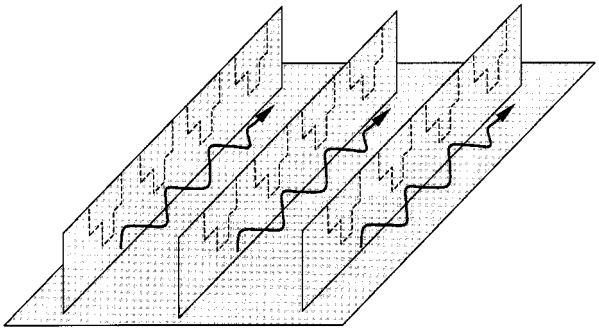

Fig. 3. Trough to support guided mode.

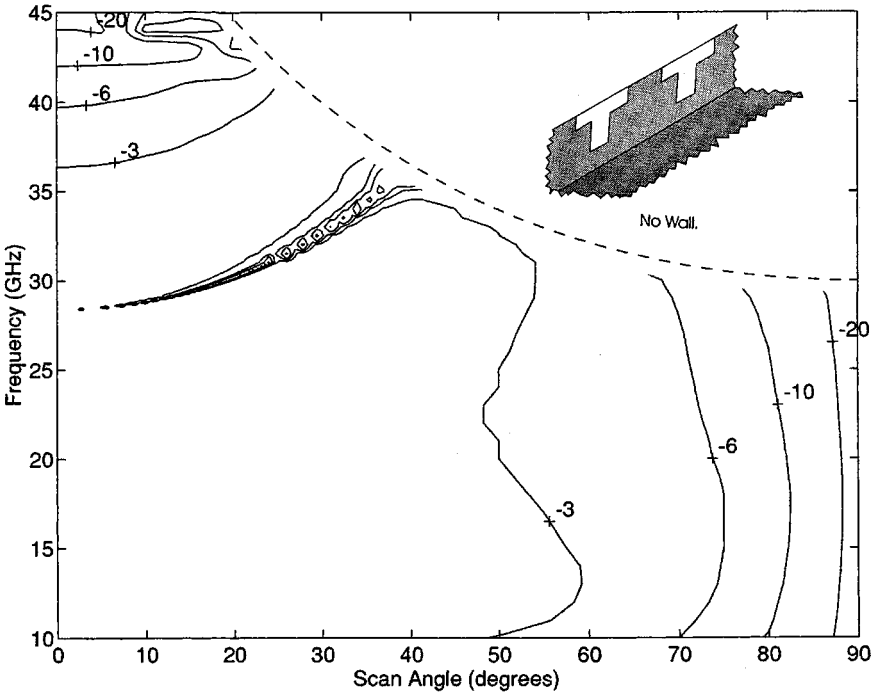

Fig. 4. Behavior of radiated power density for array without crosswalls E-plane scan. Contour lines indicate active element pattern levels of $-3, -6, -10,$ and -20 dB.

(θ_0, ϕ_0) is the scan angle and I_x^{ap} and I_y^{ap} are the unknown current coefficients. Letting both m and n go from $-N_f$ to N_f generates a set of $2(2N_f+1)^2$ basis functions for the expansion of the aperture current sheets. The results shown in this paper were obtained using $N_f = 2$ and $N_a = 30$. Convergence studies have shown (Appendix D of [10]) the numerical results to be well converged with respect to the parameters N_a and N_f.

The antenna and feedline structure used in the simulations is shown in Fig. 2. The various crosswall configurations are depicted in insets to Figs. 4 –7. Fig. 4 shows a portion of two adjacent unit cells without crosswalls. In Fig. 5, a full crosswall has been added between the unit cells. The crosswalls are electrically connected to the metallization on the substrates of the antennas. Fig. 6 shows a lower wall; a partial crosswall that contacts the ground plane and extends up to a height h. Fig. 7 shows an upper wall extending from the aperture plane toward the ground plane a distance h.

III. Broad-Band Results

In this section, the broad-band behavior of E-plane active element patterns is presented for selected crosswall arrays. The active element patterns were computed using a generator impedance of 87 Ω instead of using conjugate matching. This value gives a reasonable broadside match through a large frequency range. For these plots (see Fig. 4), the horizontal axis is E-plane scan angle in degrees and the vertical axis is frequency in gigahertz. Thus, a horizontal slice at any frequency represents an active element pattern at that frequency. For example, at 30 GHz, the active element pattern has a null due to the blindness at 19.2° and the pattern attains values of −3 dB at 55°, −6 dB at 67°, etc. For this array with E-plane spacing $= 0.5$ cm, a grating lobe can occur in the E-plane for frequencies above 30 GHz. At 30 GHz, the grating lobe occurs at −90° when the array is scanned to +90°. At 45 GHz, the grating lobe occurs at −90° when the array is scanned to 19.5°. The boundary of the region where grating lobes occur is shown on the broad-band plots as a dashed line. The region where grating lobes occur is not of interest and no contours are shown there.

Fig. 4 shows the broad-band behavior of the active element patterns for the array with no crosswalls. A scan blindness appears near broadside at 28.4 GHz and follows an arc through 19.2° at 30 GHz and 34.0° at 34 GHz. Fig. 5 shows the broad-band behavior of the active element patterns for the array with full crosswalls. No corresponding scan blindness was found for this array, further substantiating the hypothesis that a guided wave in the trough creates the blindness. The crosswalls have extended the upper frequency for which the pattern exceeds −3 dB to more than 35 GHz. However, the scan range (active element pattern $>$ −3 dB) is reduced somewhat from 50° at 25 GHz without walls to 40° with walls.

Fig. 6 shows the broad-band behavior of the active element patterns for the array with lower walls of height 0.20 cm. This height eliminates the scan blindness at 30 GHz, but a scan blindness still occurs near broadside just above 30 GHz. At 30.1 GHz the blindness occurs at 3.0°, at 31 GHz it occurs at 19.6°, at 32 GHz it occurs at 28.8°, and at 33 GHz it occurs at 37.0°. The inclusion of these lower walls creates a region from 10 to 30 GHz and from 0° to 45° that have combined mismatch and scan losses of less than 3 dB.

Fig. 7 shows the broad-band behavior of the active element patterns for the array with upper walls of height 0.02 cm. There is a blindness near broadside at about 24 GHz that moves toward endfire as frequency increases. In contrast to the lower

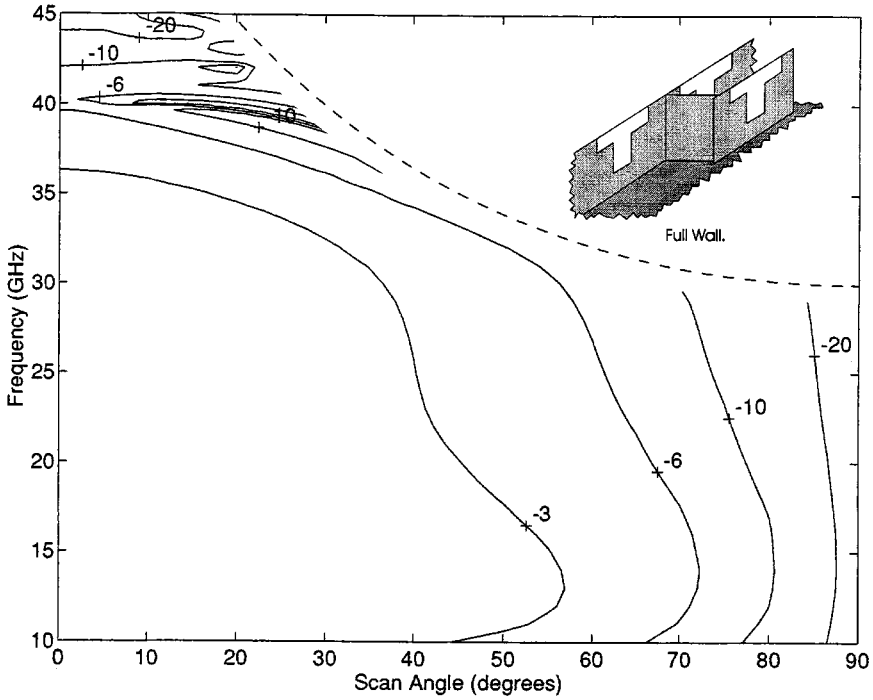

Fig. 5. Behavior of radiated power density for array with full crosswalls E-plane scan.

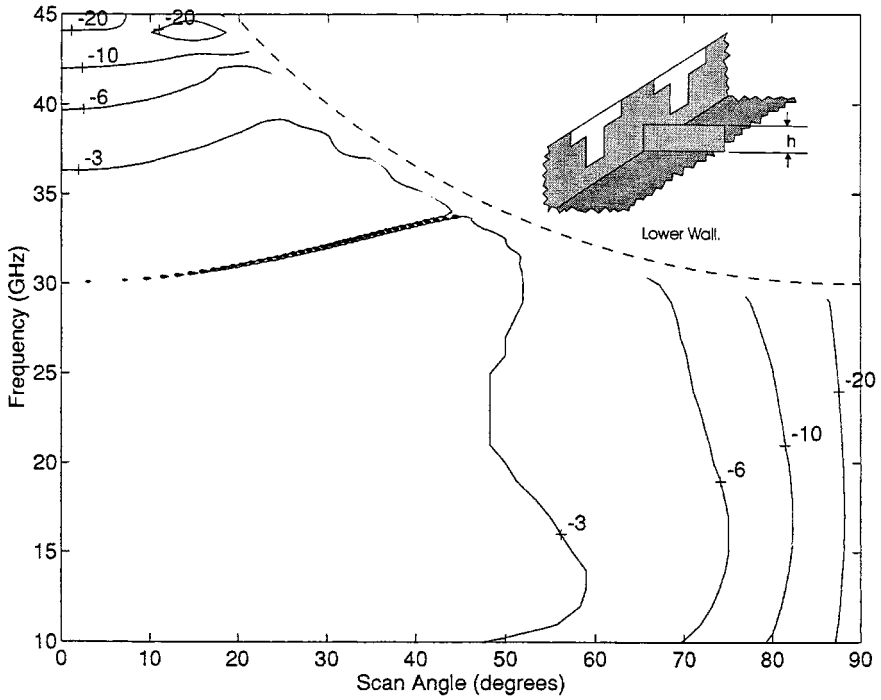

Fig. 6. Behavior of radiated power density for array with lower crosswalls $h = 0.20$ cm E-plane scan.

wall blindness, the null associated with this blindness has a very wide bandwidth and angular extent. Also, a second scan blindness appears near broadside at a frequency of 32.5 GHz.

IV. Discussion

The scan blindness reported in [7] and [8] was reproduced by using a method of moments code that can model full or partial crosswalls. If an array exhibits this scan blindness in its intended operating range, the problem can be remedied by inserting crosswalls. This substantiates the hypothesis that a trough mode causes the blindness. It was concluded in [9] that increasing the height of the lower walls moves the blindness toward broadside until it eventually disappears, whereas the broad-band results in this paper suggest a different interpretation: the blindness is pushed higher in frequency. At a fixed

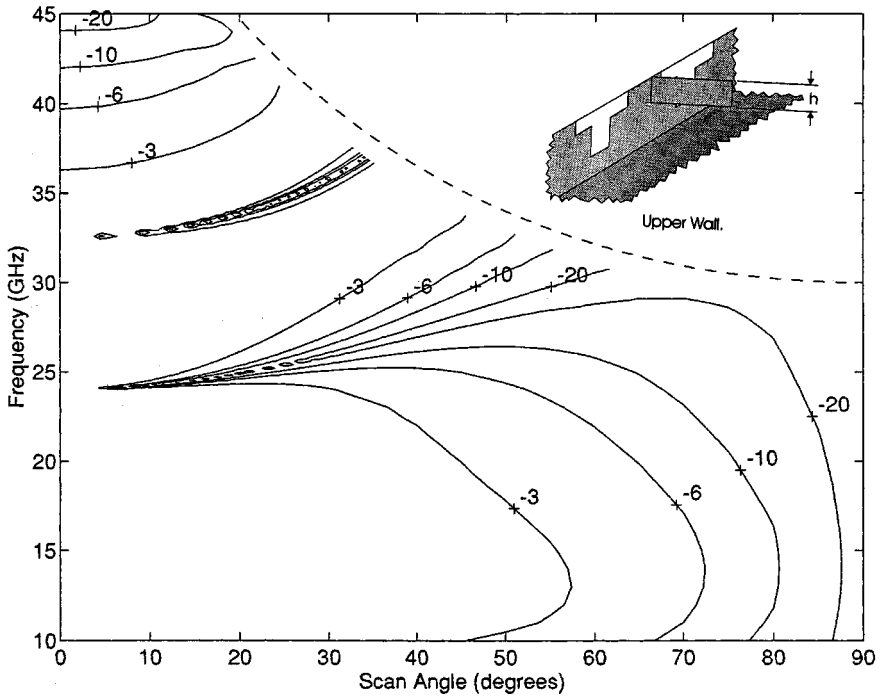

Fig. 7. Behavior of radiated power density for array with upper crosswalls $h = 0.02$ cm E-plane scan.

frequency, this results in blindnesses moving toward broadside, then disappearing. The scan blindness seen with lower walls separating the unit cells is likely due to the trough surface wave with periodic loading effects from the lower walls. Since the trough-mode blindness is not very sensitive to the shape of the tapered slot [8], the conclusions of this paper are not expected to be sensitive to the slot shape.

The broad-band results for an array with upper walls suggest that the array can be used for limited scan applications with far-out sidelobe suppression over a moderate frequency range, perhaps from 27 to 30 GHz. However, the spatial filtering characteristics change throughout this frequency range. Sidelobe suppression of 14 dB or more beyond 60° can be attained only from 28 to 30 GHz. The extra sidelobe suppression drops to just 10 dB for the 25 to 28 GHz frequency range. Also, the usable scan range drops to about 20° for the lower part of this frequency range.

The upper wall blindness occurs near broadside at 24.1 GHz. At this frequency the H-plane spacing is $a = 0.5\lambda$ and the trough width is $a - t = 0.48\lambda$. It seems unlikely that the trough surface wave is the cause of this blindness, since $a - t$ must be greater than $\lambda/2$ for this surface wave to propagate. It is more likely that this blindness is caused by some other mechanism, unknown at this time. In fact, the null depth of this blindness seems to be limited to about -25 dB. This may indicate that the phenomenon is not a true scan blindness, but rather some sort of element resonance that creates substantial, but not total, cancellation of the radiation. The computations assume lossless structures, so the finite null depth is not related to conductor or dielectric losses. Whether the null is a true blindness or some other kind of resonance, its impact on practical array designs is clearly illustrated by these results.

Changing the height of the upper wall does not eliminate the 24 GHz blindness. Arrays with $h = 0.02, 0.10, 0.20, 0.30$ and 0.498 cm all showed the blindness appearing near broadside at around 24 GHz. Varying h does affect the value of the blind frequency as a function of scan angle. With $h = 0.498$ cm, the blind frequency changes very little with scan angle, being about 26 GHz when scanned to 60°. The fact that the blindness appears with $h = 0.498$ cm (99.6% of the depth) demonstrates that good electrical contact between the ground plane and the crosswall is necessary to successfully implement a full-wall array. This also applies to arrays with lower walls.

The second blindness in Fig. 7 is likely due to the trough surface wave periodically loaded by the upper walls. This second blindness moves up in frequency as h is increased. With $h = 0.02$ cm it appears near broadside at 32 GHz, with $h = 0.10$ cm at 36 GHz, with $h = 0.20$ cm at 38 GHz, and with h greater than 0.30 cm, the blindness has moved to frequencies greater than 40 GHz.

V. Conclusion

Numerical simulations were performed on single-polarized arrays of endfire slotline antennas without crosswalls and with full-height crosswalls, lower crosswalls, and upper crosswalls. The array without crosswalls is known to have a scan blindness in the E-plane. The simulation reproduces this scan blindness and shows that the addition of full height crosswalls between the array unit cells completely eliminates this scan blindness. This finding supports the hypothesis that the blindness is caused by a trough surface wave as described in [7] and [8]. When using the full wall to eliminate the scan blindness it is important to have good electrical contact between the ground plane and the crosswall, otherwise another type of scan blindness may appear.

Arrays with partial crosswalls of the lower wall and upper wall variety were also analyzed. Lower wall arrays increase the frequency at which the scan blindness occurs. Upper wall arrays were found to have active element patterns with a somewhat different behavior. The upper wall with a height of 0.02 cm was found to have possible applications for moderate bandwidth—limited scan antennas that require far-out sidelobe suppression.

Crosswalls with other shapes may further alter the behavior of the E-plane active element patterns of these arrays and it may be possible to tailor the pattern by various shapes of partial crosswalls. Logical extensions of the crosswalls examined in this paper include various patterns of metallic walls, dielectric crosswalls, and dielectric crosswalls with printed metallic patterns.

The latter extension includes the configuration of dual-polarized endfire slotline arrays. The dual-polarized version has been suggested for electronic warfare applications [14], and for multifunction or shared aperture antennas [15].

ACKNOWLEDGMENT

The authors would like to thank Prof. R. Jackson for suggesting the study of crosswalls of various heights.

REFERENCES

[1] L. R. Lewis, M. Fassett, and J. Hunt, "A broadband stripline array element," in *Dig. 1974 IEEE Antennas Propagat. Symp.*, Atlanta, GA, pp. 335–337.

[2] P. J. Gibson, "The Vivaldi aerial," in *Proc. 9th Eur. Microwave Conf.*, Brighton, U.K., Sept. 1979, pp. 101–105.

[3] S. N. Prasad and S. Mahapatra, "A new MIC slotline aerial," *IEEE Trans. Antennas Propagat.*, vol. AP-31, pp. 525–527, May 1983.

[4] K. S. Yngvesson *et al.*, "Endfire tapered slot antennas on dielectric substrates," *IEEE Trans. Antennas Propagat.*, vol. AP-33, pp. 1392–1400, Dec. 1985.

[5] D. H. Schaubert, "Enfire slotline antennas," in *J. Int. de Nice sur les Antennes—JINA'90*, Nice, France, Nov. 1990, pp. 253–265.

[6] Y. H. Choung and C. C. Chen, "44 GHz slotline phased array antenna," in *Dig. 1991 IEEE Antennas Propagat. Symp.*, San Jose, CA, 1991, pp. 1730–1733.

[7] D. H. Schaubert and J. A. Aas, "An explanation of some E-plane scan blindnesses in single-polarized tapered slot arrays," in *Dig. 1993 IEEE Antennas Propagat. Symp.*, Ann Arbor, MI, 1993, pp. 1612–1615.

[8] D. H. Schaubert, "A class of E-plane scan blindnesses in single-polarized arrays of tapered slot antennas with a ground plane," *IEEE Trans. Antennas Propagat.*, vol. 44, pp. 954–959, July 1996.

[9] G. J. Wunsch and D. H. Schaubert, "Effects on scan blindness of full and partial crosswalls between notch antenna array unit cells," in *Dig. 1995 IEEE Antennas Propagat. Symp.*, Newport Beach, CA, 1995, pp. 1818–1821.

[10] G. J. Wunsch, "Radiation characteristics of dual-polarized notch antenna arrays," Ph.D. dissertation, Univ. Massachusetts, Amherst, Feb. 1997.

[11] P. S. Simon, K. McInturff, R. W. Jobsky, and D. L. Johnson, "Full-wave analysis of an infinite, planar array of linearly polarized, stripline-fed, tapered notch elements," in *Dig. 1991 IEEE Antennas Propagat. Symp.*, London, ON, Canada, pp. 334–337. .

[12] D. H. Schaubert, J. A. Aas, M. E. Cooley, and N. E. Buris, "Moment method analysis of infinite stripline-fed tapered slot antenna arrays with a ground plane," *IEEE Trans. Antennas Propagat.*, vol. 42, pp. 1161–1166, Aug. 1994.

[13] Y. Zilberberg, "Analysis of single polarized stripline-fed slot arrays with metallic walls," Master's thesis, Univ. Massachusetts, Amherst, Feb. 1994.

[14] J. L. Armitage, "Electronic warfare solid-state phased arrays," *Microwave J.*, pp. 109–122, Feb. 1986.

[15] J. H. Pozgay, "A wideband subarray radiator for advanced avionics applications," in *Proc. Antennas Applicat. Symp.*, Robert Allerton Park, IL, Sept. 1992.

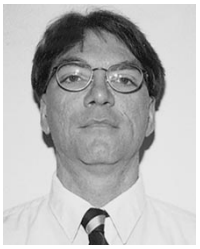

Gregory J. Wunsch received the B.S. and M.S.E.E. degrees from the University of Wisconsin, Milwaukee, in 1983 and 1991, respectively, and the Ph.D. degree in electrical engineering from the University of Massachusetts, Amherst, in 1997.

Currently, he is with Sanders, Lockheed-Martin Company, Nashua, NH, as a Principal Electrical Engineer in the Antenna and Receivers Technology Department. In 1984 he joined the Boeing Company, where he was a Product Systems Engineer, performing troubleshooting of avionics systems. From 1988 to 1991 he worked at the University of Wisconsin-Milwaukee as a Research Assistant and began specializing in electromagnetic engineering. In the summer of 1989 he worked at the Mayo Foundation, Rochester, MN, where he developed computer programs for calculating crosstalk and signal transmission. From 1991 to 1999 he worked as Research Assistant and Postdoctoral Research Associate at the University of Massachusetts, Amherst. His current research interests include antenna analysis and design and computational electromagnetics.

Daniel H. Schaubert (S'68–M'74–SM'79–F'89) has been with the University of Massachusetts, Amherst, since 1982 and is currently a Professor of electrical and computer engineering. Prior to joining the faculty at the University of Massachusetts, he was Lead Scientist for the analysis of electromagnetic problems with the National Center for Devices and Radiological Health, Rockville, MD, and was a Research Engineer with the Harry Diamond Laboratories near Washington, DC. He coedited *Microstrip Antennas* (Piscataway, NJ: IEEE Press, 1995).

Dr. Schaubert has been active in the IEEE Antennas and Propagation Society including serving as President, Vice President, two terms on the Administrative Committee, Secretary-Treasurer, Newsletter Editor, Distinguished Lecturer Program Coordinator, Associate Editor of the TRANSACTIONS ON ANTENNAS AND PROPAGATION, and chapter offices in Washington, DC. He has worked with the organizing committees of the IEEE AP-S annual symposiums and he organizes the annual Antenna Applications Symposium.